Ollscoil na Gaillimhe
University of Galway

Electro-spinning of pure collagen nano-fibres – Just an expensive way to make gelatin?

Title	Electro-spinning of pure collagen nano-fibres – Just an expensive way to make gelatin?
Author(s)	Zeugolis, Dimitrios I.;Khew, Shih T.;Yew, Elijah S.Y.;Ekaputra, Andrew K.;Tong, Yen W.;Yung, Lin-Yue L.;Hutmacher, Dietmar W.;Sheppard, Colin;Raghunath, Michael
Publication Date	2008-03-03
Publisher	Elsevier
Repository DOI	10.1016/j.biomaterials.2008.02.009

Title: Electro-spinning of pure collagen nano-fibres – Just an expensive way to make gelatin?

Authors: Dimitrios I Zeugolis[1,2,3,†], Shih T Khew[4], Elijah S Y Yew[2], Andrew K Ekaputra[2], Yen W Tong[2,4], Lin-Yue L Yung[4], Dietmar W Hutmacher[2,5,‡], Colin Sheppard[2], and Michael Raghunath[1,2,6*]

Affiliations:

[1]Tissue Modulation Laboratory, National University of Singapore (NUS), 117510, Singapore

[2]Division of Bioengineering, Faculty of Engineering, NUS, 117576, Singapore

[3]Immunology Programme, Department of Microbiology, Yong Loo Lin School of Medicine, NUS, 117456, Singapore

[4]Department of Chemical and Biomolecular Engineering, Faculty of Engineering, NUS, 117576, Singapore

[5]Department of Orthopaedic Surgery, Yong Loo Lin School of Medicine, NUS, 117597, Singapore

[6]Department of Biochemistry, Yong Loo Lin School of Medicine, NUS, 117597, Singapore

[†] Current Address: Department of Mechanical and Biomedical Engineering and National Centre for Biomedical Engineering Science, National University of Ireland Galway, Galway, Ireland

[‡] Current Address: Division of Regenerative Medicine, Institute of Health and Biomedical Innovation, Queensland University of Technology, QLD 4059, Australia

[*] Correspondence Author: Prof M Raghunath; e-mail: bierm@nus.edu.sg; Tel: +65-6516-5307; Fax: +65-6776-5322

Abstract:

Scaffolds manufactured from biological materials promise better clinical functionality, providing that characteristic features are preserved. Collagen, a prominent biopolymer, is used extensively for tissue engineering applications, because its signature biological and physico-chemical properties are retained in *in vitro* preparations. We show here for the first time that the very properties that have established collagen as the leading natural biomaterial are lost when it is electro-spun into nano-fibres out of fluoroalcohols such as 1,1,1,3,3,3-hexafluoro-2-propanol or 2,2,2-trifluoroethanol. We further identify the use of fluoroalcohols as the major culprit in the process. The resultant nano-scaffolds lack the unique ultra-structural axially periodicity that confirms quarter-staggered supramolecular assemblies and the capacity to generate second harmonics signals, representing the typical crystalline triple-helical structure. They were also characterised by low denaturation temperatures, similar to those obtained from gelatin preparations (p>0.05). Likewise, circular dichroism spectra revealed extensive denaturation of the electro-spun collagen. Using pepsin digestion in combination with quantitative SDS-PAGE, we corroborate great losses of up to 99% of triple-helical collagen. In conclusion, electro-spinning of collagen out of fluoroalcohols effectively denatures this biopolymer, and thus appears to defeat its purpose, namely to create biomimetic scaffolds emulating the collagen structure and function of the extracellular matrix.

Keywords: collagen denaturation; gelatin; denaturation temperature; second harmonic generation, transmission electron microscopy; circular dichroism

Running Head: Collagen denaturation through electro-spinning

1. Introduction

Collagen type I accounts for up to 70-90% of the collagen found in the body and it is present in the form of elongated fibres in various tissues. Individual fibrils can be greater than 500μm in length and 500nm in diameter [1, 2]. These building blocks are rod-like triple-helices that are stabilised by intra-molecular hydrogen bonds between Gly and Hyp in adjacent chains [3-6]. Tissues rich in fibrous collagen such as skin and tendon are generally used to extract collagen. Dilute acidic solvents are used to break intermolecular cross-links of the aldimine type, whilst proteolytic enzymes, such as pepsin, are used to cleave the more stable cross-links of the keto-imine type. Pepsin cleaves only the non-triple-helical C- and N-telopeptides, leaving the triple-helical molecule intact [7-9]. Extracted collagen from either of the above preparations is favoured for biomedical applications since *in vitro*, under appropriate conditions, would spontaneously self-assemble to form biodegradable and biocompatible insoluble fibrils of high mechanical strength, low immunogenicity and with a D-periodicity indistinguishable from that of native fibres [10-14].

Electro-spinning has been recently introduced as the most promising technique to manufacture *in vitro* fibrous scaffolds for tissue engineering application with fibre diameter ranging from a few microns to less than 100nm. Such materials aim to mimic extracellular matrix components, such as collagen fibrils whose diameter *in vivo* range from 20nm to 40μm [15-17]. Currently, the most widely adopted method involves the electro-spinning of pure collagen or collagen-poly(ε-caprolactone) blends out of highly volatile fluoroalcohols such as 1,1,1,3,3,3-hexafluoro-2-propanol (HFP) [18-25] or 2,2,2-trifluoroethanol (TFE) [24, 26]. However, it has been shown earlier with non-collagenous proteins that fluoroalcohols not only denaturate the native structure, but also lower the denaturation temperature [27-29]. Moreover, in a recent publication, it was shown that 45% of collagen is apparently lost during electro-spinning [30]. Additionally, electro-spinning of collagen using either HFP or TFE has been reported repeatedly to yield collagen nano-fibres that do not swell when in aqueous media like other collagenous structures [31-33], but instead are readily soluble in water, tissue fluids or blood [20, 22, 24, 34-36]. Since gelatin is the water-soluble degradation product of the originally water-insoluble collagen fibril [37], the observed water solubility of the electro-spun collagen scaffolds might point to an extensive conformational change. Given the above, our hypothesis was that through the electro-spinning process, denaturation of collagen takes place and gelatin is created.

To verify our hypothesis, we conducted a series of specific experiments that distinguish collagen from gelatin. Collagen is a crystalline [38-41] (Second Harmonic Generation Experimentation), triple helical molecule [2-6, 31] (Circular Dichroism Experimentation), whilst gelatin is characterised by destroyed α-chains, disrupted triple-helical and fibrillar structure and lacking internal structure or configurational order [37]. Moreover, the collagen fibrils possess a high degree of axial alignment and exhibit a characteristic D banding (the finger print of fibrous collagens), which results from alternating overlap and gap zones, produced by the specific packing arrangement of the 300nm long and 1.5nm wide collagen molecules. This produces an average periodicity of 67nm in the native hydrated state [1, 3, 4, 12, 14, 31, 33, 42-45], although dehydration and shrinkage during conventional sample preparation for Transmission Electron Microscopy results in lower values of around 55 to 65nm [1, 44] (Transmission Electron Microscopy Experimentation). Furthermore, the denaturation temperature of collagen is higher than the denaturation temperature of gelatin [31, 46-52] (Differential Scanning Calorimetry Experimentation). Most importantly, the tight triple helical structure of the collagen molecule makes it resistant to pepsin or trypsin, unless its folding is locally compromised by either point mutations or heat denaturation [53] (Pepsin Digestion and SDS-PAGE Experimentation). Such molecules are unstable at physiological temperatures and they are degraded intra-cellularly [14]. Based on all the above, we demonstrate for first time that the electro-spun collagen scaffolds are not crystalline; are not triple-helical; are not quarter-staggered arranged; have denaturation temperature lower than or similar to gelatin; and are pepsin susceptible. Freeze-dried collagen dissolved in HFP and freeze-dried again (HFP-recovered collagen) also exhibited similar properties with those obtained from gelatin preparations, clearly indicating that fluoroalcohols are the major cause of denaturation. Taken together, this builds up strongest evidence that electro-spinning of collagen or co-spinning of collagen-synthetic polymers out of fluoroalcohols results in the creation of gelatin, a protein derived from denatured collagen and is characterised by destroyed α-chains, disrupted triple-helical and fibrillar structure and lacking internal structure or configurational order [37].

2. Materials & Methods

2.1. Materials

Porcine skin type A and bovine type B gelatin were obtained from Sigma-Aldrich (Singapore). Purified type I freeze-dried bovine dermal atelocollagens were obtained from Koken Co. (Japan) and Symatese Biomateriaux (France). In-house type I atelocollagen from porcine Achilles tendon was extracted as has been described previously [54]. Medical grade poly(ε-caprolactone) (mPCL) was purchased from Birmingham Polymers Inc (USA). Rat tail tendons and normal human skin were used as representatives of native assemblies. Unless noted otherwise, all chemicals and reagents were purchased from Sigma-Aldrich (Singapore).

2.2. Nano-fibre fabrication through electro-spinning

Typical protocols for the electro-spinning were used based on previous publications [18, 19, 21, 24]. The following preparations were investigated: (a) in-house, Koken and Symatese collagens and Sigma gelatin type A and B dissolved in HFP at 50mg/ml concentration; (b) Koken collagen dissolved in HFP and TFE at 180mg/ml concentration; and (c) in order to investigate whether blending and consequent co-spinning of collagen with mPCL could prohibit or restrict the denaturation of collagen mPCL-Symatese collagen and mPCL-Sigma gelatin type A and B blends (5 to 1 ratio) and mPCL dissolved in HFP at 125mg/ml concentration. Either of the above solutions was loaded into a syringe pump (KD-Scientific, USA), which was set at 0.75 to 1.2ml/h. Upon application of high voltage (10 to 15KV; applied current was below 1μA) (Gamma High Voltage Research, USA) between the syringe needle (internal diameter 27G1/2) and the aluminium collector (12 to 15cm distance), the solvent was evaporated and the nano-fibres were deposited on the collector. All experiments were carried out at room temperature (RT: 22-26^{0}C) and 55-73% relative humidity.

2.3. HFP-recovered collagen

In order to assess the effect of the fluoroalcohols alone on collagen structure, freeze-dried in-house, Koken and Symatese type I collagen preparations were dissolved in HFP (50mg/ml concentration) and freeze-dried (Advantage ES-53, VirTis, SP Industries, Inc., USA). The material obtained is referred to as HFP-recovered collagen.

2.4. Micro-fibre fabrication through extrusion

The procedure for fibre formation has been described in detail previously [54] based on previous publications [55, 56]. Briefly, a solution of in-house collagen (6mg/ml in 0.5M acetic acid) was extruded into the Fibre Formation Buffer (FFB) comprised of 118mM phosphate buffer and 20% polyethylene glycol Mw 8,000 at pH 7.55 and 37^{0}C at a flow rate of 0.4ml/min. Resultant fibres were allowed to remain in this buffer for a maximum period of 10min, followed by further 10min incubation in 6.0mM phosphate buffer and 75mM NaCl at pH 7.10 and 37^0C and further 10min incubation in distilled water at RT. Finally the fibres air-dried under the tension of their own weight at RT.

2.5. Self-assembly of collagen

For the self-assembly experiments, freeze-dried collagens from in-house, Koken and Symatese preparations and their HFP-recovered counterparts were dissolved in 0.5M acetic acid at 1mg/ml concentration. FFB (see above) was warmed up for 30 min at 35^0C and was mixed with either of the collagen preparations (ratio of FFB to collagen solution 3 to 2). The mixture was incubated for 48h at 35^0C.

2.6. Scanning Electron Microscopy (SEM)

The morphology of the produced scaffolds was evaluated using a QuanTA 200F Jeol Scanning Electron Microscope (FEI Company, Hillsbora, Oregon-USA) after gold sputtering with a Jeol JFC-1600 Auto Fine Coater (Tokyo, Japan).

2.7. Transmission Electron Microscopy (TEM)

Rat tail tendon, extruded collagen fibres and electro-spun scaffolds were fixed in 2.5% glutaraldehyde in 0.1M phosphate buffer for 16h at RT. After osmication and dehydration through a series of ascending aqueous ethanol concentrations, samples were embedded in araldite using appropriate intermediate infiltration steps. Ultra-thin sections were obtained using a Reichert Ultracut E ultra-microtome (Leica Microsystems Ltd, Germany), collected on Formvar coated copper grids and were viewed with a JEM-1220 Transmission Electron Microscope (JEOL Ltd, Japan) at 80KV, after were contrasting with 1% phosphotungstic acid pH 7.4 for 10sec and with aqueous 2% uranyl acetate solution for 10min. Collagen self-assemblies were analysed without fixation and embedding. 20μl of the assembly solution were transferred onto Formvar coated grids blotted against filter paper to remove excess water, dried for 16h at RT and contrasted as described above prior to viewing.

2.8. Second Harmonic Generation (SHG)

Second harmonic microscopy was performed by coupling a Titanium-Sapphire laser (Mira 900, Coherent, USA) to an upright microscope (IX71, Olympus, Japan). The laser was tuned to 838nm (<200femtosecond, 76MHz) and scanning was done with the commercial FV300 (Olympus, Japan). The beam was such that it slightly under-filled the back-aperture of the 20x objective and the input power was <100mW. Collection of the SHG signals was done in transmission with an oil immersion condenser and spectral filtering of the signal was carried out using a band-pass filter (BG40, Schott, Germany) and a short-pass filter passing below 450nm (FES450, Thorlabs, USA). Imaging was controlled with the Fluoview 5.0b software (Olympus, Japan) and images were scanned at 512x512 pixels and averaged over 4 images depending on the noise levels. Nano-scaffolds, freeze-dried materials and 5μm thick cryosections (CM3050S, Leica Microsystems Ltd, Germany) of rat-tail tendon, normal human skin and extruded collagen fibres were mounted on glass-slides using polyvinyl-alcohol-DABCO medium underneath glass-coverslips to retain the materials wet prior to SHG investigation.

2.9. Differential Scanning Calorimetry (DSC)

The denaturation temperature was determined using an 822e Mettler-Toledo differential scanning calorimeter (Mettler-Toledo International Inc., Singapore). 50mg of either preparation was hydrated in 1500μl of PBS. The following day, the samples were blotted with filter paper to remove excess water. 5 to 15μg wet weight samples of every preparation were hermetically sealed in 50μl aluminium pans and heated at a constant temperature ramp of 5^0C/min in the temperature range of 15 to 90^0C. An empty aluminium pan was used as reference probe. Thermal denaturation, the endothermic transition, was recorded as a typical peak, and two characteristic temperatures were measured corresponding to the peak (temperature of maximum power absorption during denaturation) and onset (temperature at which the tangent to the initial power versus temperature line crosses the baseline) temperatures.

2.10. Sodium Dodecyl Sulfate-Polyacrylamide Gel Electrophoresis (SDS-PAGE)

Freeze-dried materials (original and HFP-recovered), extruded collagen micro-fibres and electro-spun nano-fibres were subjected to acid-solubilisation in 0.5M acetic acid or pepsin-digestion in 0.1mg pepsin per ml of 0.5M acetic acid (1mg/ml concentration in either case). Obtained suspensions were centrifuged for 15min at 13,326g at 4^0C (Biofuge, Fresco Heraeus Instruments, Germany) and the supernatants were analysed using SDS-PAGE. Protein bands were visualised using silver-staining (SilverQuest™ Kit, Invitrogen, Singapore) and quantitated using a GS-800 densitometer (BioRad, USA).

2.11. Circular Dichroism (CD)

CD measurements of extracted material (see above) were performed using a Jasco Model J-810 spectropolarimeter (Jasco, UK) using a quartz cylindrical cuvette (Hellma, Germany) with a path length of 0.1mm. The cuvette was filled with 150μl of sample for each measurement. CD spectra were obtained by continuous wavelength scans (average of three scans) from 180 to 260nm at a scan-speed of 50nm/min. The samples were equilibrated for an hour at RT before the CD spectrum was acquired.

2.12. Statistical Analysis

Numerical data is expressed as mean ± SD. Analysis was performed using statistical software (MINITAB^{TM} version 13.1, Minitab, Inc.). One way analysis of variance (ANOVA) for multiple comparisons and 2-sample t-test for pair wise comparisons were employed after confirming the following assumptions: (a) the distribution from which each of the samples was derived was normal (Anderson-Darling normality test); and (b) the variances of the population of the samples were equal to one another (Bartlett's and Levene's tests for homogenicity of variance). Non-parametric statistics were utilised when either or both of the above assumptions were violated and consequently Kruskal-Wallis test for multiple comparisons or Mann-Whitney test for 2-samples were carried out. Statistical significance was accepted at $p<0.05$.

3. Results

3.1. Scanning Electron Microscopy

Figure 1 demonstrates SEM micrographs of the scaffolds evaluated in this study. It is apparent that electro-spinning yielded a randomly orientated and interconnected fibrous mesh, with individual fibre diameter to be in the nano-meter range. Through self-assembly, a thicker in diameter fibrous lattice was produced. The extrusion of collagen into a neutral buffer solution resulted in micro-scale fibres with smooth surface morphology and diameter similar to those of native rat-tail tendon.

3.2. Transmission Electron Microscopy

The electro-spun nano-fibres, independent of the collagen source, did not exhibit the characteristic cross-striation pattern of collagen that was apparent for the self-assembled and extruded collagen fibres and the native rat tail tendon fibres (Figure 2). Self-assemblies from HFP-recovered collagen exhibited the characteristic quarter-stagger arrangement of collagen only inconsistently (Figure 2).

3.3. Second Harmonic Generation

Native tissues generated stronger harmonic signals than the extruded and self-assembled collagen fibres and freeze-dried collagen (Figure 3). In contrast, neither the HFP-recovered collagens, nor the nano-fibres of collagen, gelatin or blends of thereof with mPCL, independent of the solvent utilised for the electro-spinning process, exhibited any SHG signals (Figure 3).

3.4. Differential Scanning Calorimetry

Table 1 provides the hydrothermal stability of the rehydrated materials. It is noteworthy that during rehydration, the starting freeze-dried collagens and extruded collagen fibres swelled, whilst the HFP-recovered and the electro-spun collagen-derived nano-fibres formed gels similar to those obtained from the gelatin preparations (results not shown). Extruded collagen fibres exhibited improved thermal properties over the original freeze-dried material (p<0.015 and p<0.016 for enthalpy and temperature of denaturation respectively), higher than any HFP-recovered collagen preparation ($p<0.007$ and $p<0.001$ for enthalpy and temperature of denaturation respectively) or pure protein ($p<0.008$ and $p<0.001$ for enthalpy and temperature of denaturation respectively) nano-scaffold, and were found to closely match those of a native tissue ($p>0.05$ and $p<0.003$ for enthalpy and temperature of denaturation respectively), rat tail tendon in that case. HFP-recovered collagen ($p<0.009$ and $p<0.001$ for enthalpy and temperature of denaturation respectively) and electro-spun scaffolds ($p<0.004$ and $p<0.001$ for enthalpy and temperature of denaturation respectively) demonstrated impaired thermal properties over their original freeze-dried counterparts, independent of the solvent utilised. Moreover, collagen-derived nano-fibres and HFP-recovered collagen preparations exhibited enthalpies of denaturation similar ($p>0.05$) or even inferior ($p<0.006$) to those of gelatin.

3.5. Circular Dichroism

Figure 4 presents the CD spectra of the different preparations. The acid-solubilised and pepsin-digested freeze-dried collagens exhibited sinusoidal CD spectra typical for triple-helical collagen in solution, consisted of a negative band with peak at around 198nm, a cross-over at 214nm and a positive band with peak at around 222nm. Gelatin exhibited only a negative peak of lower molar ellipticity than collagen, a characteristic of random conformation of the α-chains. The CD spectra of acid-solubilised electro-spun nano-fibres and HFP-recovered material were shifted to the right with a cross-over at around 218nm, demonstrated a negative band of low molar ellipticity and either lacked the positive peak alike the gelatin preparations; or showed a positive peak of very low intensity at around 222nm. The pepsin-digested complements of the above samples were shifted to the left with a cross-over at around 208nm, a negative band of low intensity and a positive band with maximum molar ellipticity at around 218nm. Extruded collagen fibres (collagen supramolecular assemblies), being acid-solubilisation and pepsin-digestion resistant (insoluble), did not exhibit any peaks (See Supplementary information, Figure S1).

3.6. Sodium Dodecyl Sulfate-Polyacrylamide Gel Electrophoresis

The protein-band pattern of Symatese collagen and Sigma gelatin type B (Figure 5) provides an example of the degree of purity of the original freeze-dried materials. The freeze-dried collagen was found to be resistant to peptic digest, showing its intact triple-helical nature, whilst the Sigma gelatin type B preparations were abolished from the gels, demonstrating absolute destruction of the randomly coiled α-chains. The densitometric analysis of the Symatese collagen preparations (Table 2) revealed a loss in collagen α_{1+2}(I) chains of around 58.2% for the HFP-recovered materials, which was increased up to 64.2% reduction for α_{1+2}(I) when the collagen was electro-spun into nano-fibres. Almost no collagen was detectable, when complementary analysis of the pepsin-digested samples was carried out; 93% losses for the α_{1+2}(I) for the HFP-recovered collagen and 99.5% losses for the α_{1+2}(I) for the electro-spun nano-fibres. Analogous losses were obtained with the HFP-recovered and the electro-spun nano-scaffolds preparations originated from in-house collagen; the extruded however collagen fibres, being resistant (insoluble) to acid-solubilisation and pepsin-digestion exhibited clear lanes (Figure 6). Evaluation of Koken collagen originated nano-scaffolds derived from TFE, proportional losses as with those obtained from HFP were obtained (Figure 7). Blends of mPCL-Symatese Collagen or mPCL-Sigma gelatin type A showed a comparable degree of protein denaturation after electro-spinning (Figure 8).

4. Discussion

Since electro-spinning is currently the prime method to construct nano-fibrous scaffolds and collagen is a superior, clinical approved biopolymer, it appeared logical to combine both technology and biomaterial to fabricate submicron scaffolds for tissue engineering applications. After Huang *et al.* 2001 [57] showed the feasibility to electro-spin collagen, this approach has become popular in the biomaterials and tissue engineering field, as reflected in a recent steep rise of publications. However, every single article testifies that collagen scaffolds derived via electro-spinning are readily soluble in aqueous media. Remarkably, this abnormal transformation of the water-insoluble biopolymer into a water-soluble scaffold was never questioned. Instead, it became customary to remedy the instability of the collagen nano-fibres by chemical [19, 20, 34, 35, 58] or physical [36] cross-linking. Based on our comprehensive work, we present unambiguous evidence that electro-spinning degrades collagen into gelatin, which explains the solubility in aqueous media.

Starting on the ultra-structural level, we confirmed the presence of collagen-typical periodicity for native rat tail tendon, self-assembled and extruded collagen fibres, which results from alternating overlap and gap zones, produced by the specific packing arrangement of the 300nm long and 1.5nm wide collagen triple helices [1, 3, 44]. It has been recognised for over 50 years that solutions of extracted collagen, when the pH, temperature and ionic strength are adjusted to physiological values, will spontaneously self-assemble to form insoluble, axially ordered fibrillar structures with characteristic cross-striated banding pattern [1, 44, 59-63]. The ability of type I collagen to form striated fibrils involves specific charge-charge and hydrophobic interactions. Although the mechanism of fibril formation *in vitro* and *in vivo* may be different, the final products have similar banding patterns [13]. Therefore, the inconsistent presence of periodic pattern for the HFP-recovered collagen and the total lack for the electro-spun collagen scaffolds suggest compromised supramolecular collagen structure. This finding is in contrast to earlier work [18, 22] presenting cross-striated electro-spun nano-fibres. As revealed from the SDS-PAGE results, a small amount of collagen can withstand the process and therefore, we cannot exclude the possibility that this small fraction of intact triple-helices might form infrequently cross-striated fibrils, as also observed with the HFP-recovered collagen. However, this merely underlines the loss of integrity of the starting material.

Optical analysis using second harmonic generation corroborated the ultra-structural data. The collagen fibril has been described as essentially a long, thin, single crystal [64] and X-ray diffraction studies indicate that the collagen molecules are arranged on a three-dimensional crystalline lattice [38, 39, 65, 66] that, *in vivo*, can be highly polarisable and often assembles into large, ordered noncentrosymmetric structures [67, 68]. Its unique triple-helical structure and the high levels of crystallinity make collagenous structures exceptionally efficient in generating the second harmonic of incident light [69, 70]. An excellent example is rat tail tendon, a tissue rich in type I collagen with extremely high level of crystallinity and structural alignment that is characterised by strong SHG signals in the presence of intense laser light [69]. Using native rat tail tendon and human skin as positive controls, we confirmed SHG signals in freeze-dried collagens and self-assembled collagen fibres, and as a novel finding, in extruded collagen fibres. The intensity of the signals in our *in vitro* collagen assemblies was lower in comparison to native tissues. Although this has been observed previously [70, 71], our TEM findings pinpoint the intensity difference between the *in vitro* and *in vivo* assemblies to the low and high respectively supramolecular configuration order. Gelatin on the other hand, our benchmark structure of thermally destroyed collagen, did not exhibit second harmonics, as also has been observed earlier [72, 73]. Accordingly, the absence of SHG signals in assemblies of HFP-recovered collagen and electro-spun collagen nano-fibres strongly suggests destruction of the microcrystalline structure of collagen.

Another indication of denaturation of collagen through electro-spinning using fluorinated alcohols was derived from the thermal analysis. When collagen in hydrated state is heated, the helix-coil transition takes place, during which the triple helix melts and progressively dissociates into the three randomly coiled peptide α-chains (gelatin) [31, 46, 48, 49]. As expected, collagen with intact triple-helical conformation, such as the freeze-dried collagen and the extruded collagen fibres exhibited thermal features comparable to native tissue that would not melt at physiological temperatures. However, the HFP-recovered and the electro-spun collagen-originated nano-fibres exhibited thermal profiles comparable to those of gelatin, suggesting complete denaturation [31, 50-52].

Further biophysical analysis of the nano-fibres in solutions showed extended denaturation of the triple-helical collagen, which is in agreement with a recent publication [30]. The CD spectra of the freeze-dried collagen preparations were consistent with the characteristic sinusoidal collagen triple-helical structure [74-76]. In contrast, HFP-recovered collagen and the electro-spun collagen originated scaffolds exhibited CD spectra indicating massive loss of triple-helical collagen [75]; or suggesting random coils similar to those obtained from gelatin [52, 74, 76] respectively. When the same preparations were subjected to peptic digest, the CD spectra shifted to the left, indicating a non-triple-helical conformation, as has been observed with charged polypeptides, such as polylysine at low pH [76, 77].

Finally, quantitative SDS-PAGE allowed us to determine the loss of triple-helical collagen during the subsequent electro-spinning steps. As identical amounts of dry weight of freeze-dried collagen (starting material), HFP-recovered collagen or electro-spun fibres were subjected to SDS-PAGE analyses, a direct comparison of collagen content of the different samples was possible. Under these conditions, an apparent 58% and 64% reduction in collagen content for the HFP-recovered collagen and for the electro-spun scaffolds respectively was observed under acid solubilisation. These results are in accordance with a recent publication, where, using CD, a 45% loss in triple-helical collagen was observed for the electro-spun nano-fibres [30]. Although this test already indicates extensive losses of the starting material, it does not allow us to decide whether the α-bands seen in the gel have been derived from intact or denatured triple-helices. We therefore applied the most stringent test of triple-helical integrity, namely the probing of collagen with pepsin. Pepsin is an aggressive protease that destroys globular proteins easily, but cannot attack an intact collagen type I triple-helix, unless it is partially unfolded, molten or broken [78]. Therefore, SDS-PAGE *after* peptic digest demonstrated that in-house, Koken and Symatese type I collagen preparations were comprised of α-chains of an intact collagen triple helix, whilst Sigma gelatin type A and B preparations were completely destroyed. Using this biochemical method, we were able to reveal the full and true extent of the collagen denaturation during the electro-spinning process. Disassociation of Symatese type I collagen in HFP resulted in 93% collagen losses, whilst the consequent application of high voltage yielded nano-scaffolds with approximately 0.5% collagen content (99.5% collagen losses). These results were consistent for all collagen preparations, independent of the fluoroalcohol used for the electro-spinning (HFP or TFE). Moreover, co-spinning of collagen-mPCL did not protect in any way the triple-helical structure of collagen and proportional losses occurred. Overall, our data demonstrates that extensive denaturation takes place upon disassociation of collagen in the solvent, which is in direct agreement with previous published reports showing that fluoroalcohols denature the native structure of proteins [27-29]. It is worth pointing out that SDS-PAGE data of electro-spun collagen-originated scaffolds have been reported twice previously. However, no comparison with the starting material was available in the first publication [22]; and conspicuous losses in the second were not commented [58]. We believe that the peptic challenge of electro-spun collagen is the most stringent biochemical test and we have little doubt that the application of it in either of the earlier works, would have unravelled the damage that was done to the starting material.

5. Conclusion

Electro-spinning of collagen out of fluoroalcohols denatures collagen to gelatin. Thus, this in the literature so highly advocated process for fabrication of collagen nano-scaffolds appears to defeat its purpose, namely to preserve the typical biological properties of collagen and to imitate this major part of the extracellular matrix. Hence, if the unique properties of triple-helical collagen are desired within the design, then coating of the electro-spun scaffolds with collagen is the method of choice.

6. Acknowledgments

The authors are grateful to Peng Yanxian, Clarice Chen and Shaoping Zhong for technical support; and Dr Ricky R Lareu for his constructive discussion. This work was supported by grants (R-397-000-025-112 and R-279-000-168-712) of the Faculty Research Committee of the Faculty of Engineering, National University of Singapore.

7. References

1. Kielty CM, Grant ME. The collagen family: Structure, assembly and organization in the extracellular matrix. In: Royce PM, Steinmann B, editors. Connective Tissue and Its Heritable Disorders: Molecular, Genetic and Medical Aspects. 2nd ed. New York: John Wiley Inc, 2002. p. 159-221.

2. Ramshaw JAM, Werkmeister JA, Glattauer V. Collagen-based Biomaterials. Biotechnology and Genetic Engineering Reviews 1995;13:335-382.

3. van der Rest M, Garrone R, Herbage D. Collagen: A family of proteins with many facets. In: Kleinman HK, editor. Advances in molecular and cell biology: JAI Press Inc, 1993. p. 1-67.

4. Hulmes DJS, Miller A, Parry DAD, Piez KA, Woodhead-Galloway J. Analysis of the primary structure of collagen for the origins of molecular packing. Journal of Molecular Biology 1973;79:137-148.

5. Paul RG, Bailey AJ. Chemical stabilisation of collagen as a biomimetic. The Scientific World Journal 2003;3:138-155.

6. Bailey AJ, Paul RG. Collagen: A not so simple protein. Journal of the Society of Leather Technologists and Chemists 1998;82:104-110.

7. Light ND. Collagen in skin: Preparation and Analysis. In: Skerrow D, Skerrow CJ, editors. Methods in Skin Research: John Wiley & Sons Ltd, 1985. p. 559-586.

8. Gelman RA, Poppke DC, Piez KA. Collagen fibril formation in vitro. The role of the nonhelical terminal regions. Journal of Biological Chemistry 1979;254:11741-11745.

9. Friess W. Collagen - biomaterial for drug delivery. European Journal of Pharmaceutics and Biopharmaceutics 1998;45:113-136.

10. Lynn AK, Yannas IV, Bonfield W. Antigenicity and immunogenicity of collagen. Journal of Biomedical Materials Research Part B-Applied Biomaterials 2004;71B:343-354.

11. Hsu S, Jamieson AM, Blackwell J. Viscoelastic studies of extracellular matrix interactions in a model native collagen gel system. Biorheology 1994;31:21-36.

12. Holmes DF, Graham HK, Trotter JA, Kadler KE. STEM/TEM studies of collagen fibril assembly. Micron 2001;32:273-285.

13. Silver FH, Birk DE. Molecular structure of collagen in solution: comparison of types I, II, III and V. International Journal of Biological Macromolecules 1984;6:125-132.

14. Hulmes DJS. The collagen superfamily--diverse structures and assemblies. Essayes in Biochemistry 1992;27:49-67.

15. Jarvinen T, Jarvinen T, Kannus P, Jozsa L, Jarvinen M. Collagen fibres of the spontaneously ruptured human tendons display decrease thickness and crimp angle. Journal of Orthopaedic Research 2004;22:1303-1309.

16. Huang Y, Meek KM, Ho M-W, Paterson CA. Anaylsis of Birefringence during Wound Healing and Remodeling following Alkali Burns in Rabbit Cornea. Experimental Eye Research 2001;73:521-532.

17. Silver FH, Freeman JW, Seehra GP. Collagen self-assembly and the development of tendon mechanical properties. Journal of Biomechanics 2003;36:1529-1553.

18. Matthews JA, Wnek GE, Simpson DG, Bowlin GL. Electrospinning of Collagen Nanofibers. Biomacromolecules 2002;3:232-238.

19. Li M, Mondrinos MJ, Gandhi MR, Ko FK, Weiss AS, Lelkes PI. Electrospun protein fibers as matrices for tissue engineering. Biomaterials 2005;26:5999-6008.

20. Rho KS, Jeong L, Lee G, Seo B-M, Park YJ, Hong S-D, Roh S, Cho JJ, Park WH, Min B-M. Electrospinning of collagen nanofibers: Effects on the behavior of normal human keratinocytes and early-stage wound healing. Biomaterials 2006;27:1452-1461.

21. Shih Y-RV, Chen C-N, Tsai S-W, Wang YJ, Lee OK. Growth of Mesenchymal Stem Cells on Electrospun Type I Collagen Nanofibers. Stem Cells 2006;24:2391-2397.

22. Telemeco TA, Ayres C, Bowlin GL, Wnek GE, Boland ED, Cohen N, Baumgarten CM, Mathews J, Simpson DG. Regulation of cellular infiltration into tissue engineering scaffolds composed of submicron diameter fibrils produced by electrospinning. Acta Biomaterialia 2005;1:377-385.

23. Zhong S, Teo WE, Zhu X, Beuerman RW, Ramakrishna S, Yung LYL. An aligned nanofibrous collagen scaffold by electrospinning and its effects on in vitro fibroblast culture. Journal of Biomedical Materials Research Part A 2006;79A:456-463.

24. Zhang YZ, Venugopal J, Huang ZM, Lim CT, Ramakrishna S. Characterization of the surface biocompatibility of the electrospun PCL-collagen nanofibers using fibroblasts. Biomacromolecules 2005;6:2583-2589.

25. Kwon IK, Matsuda T. Co-Electrospun Nanofiber Fabrics of Poly(L-lactide-co-*e*-caprolactone) with Type I Collagen or Heparin. Biomacromolecules 2005;6:2096-2105.

26. Zhong S, Teo WE, Zhu X, Beuerman R, Ramakrishna S, Yung LY. Formation of collagen-glycosaminoglycan blended nanofibrous scaffolds and their biological properties. Biomacromolecules 2005;6:2998-3004.

27. Hong D-P, Hoshino M, Kuboi R, Goto Y. Clustering of fluorine-substituted alcohols as a factor responsible for their marked effects on proteins and peptides. J Am Chem Soc 1999;121:8427-8433.

28. Cort JR, Andersen NH. Formation of a Molten-Globule-like State of Myoglobin in Aqueous Hexafluoroisopropanol. Biochemical and Biophysical Research Communications 1997;233:687-691.

29. Kundu A, Kishore N. 1,1,1,3,3,3-hexafluoroisopropanol induced thermal unfolding and molten globule state of bovine alpha-lactalbumin: calorimetric and spectroscopic studies. Biopolymers 2004;73:405-420.

30. Yang L, Fitie CFC, van der Werf KO, Bennink ML, Dijkstra PJ, Feijen J. Mechanical properties of single electrospun collagen type I fibers. Biomaterials 2008;29:955-962.

31. Bailey AJ. Procter memorial lecture Collagen-Nature`s framework in the medical, food and leather industries. Journal of the Society of Leather Technologists and Chemists 1992;76:111-127.

32. Finch A, Gardner PJ, Ledward DA, Menashi S. The thermal denaturation of collagen fibres swollen in aqueous solutions of urea, hexamethylenetetramine, p-benzoquinone and tetra-alkylammonium salts. Biochimica et Biophysica Acta (BBA) - Protein Structure 1974;365:400-404.

33. Friess W, Lee G. Basic thermoanalytical studies of insoluble collagen matrices. Biomaterials 1996;17:2289-2294.

34. Buttafoco L, Kolkman NG, Engbers-Buijtenhuijs P, Poot AA, Dijkstra PJ, Vermes I, Feijen J. Electrospinning of collagen and elastin for tissue engineering applications. Biomaterials 2006;27:724-734.

35. Zhong SP, Teo WE, Zhu X, Beuerman R, Ramakrishna S, Yung LYL. Development of a novel collagen–GAG nanofibrous scaffold via electrospinning. Materials Science and Engineering: C 2007;27:262-266.

36. Kidoaki S, Kwon IKIK, Matsuda T. Mesoscopic spatial designs of nano- and microfiber meshes for tissue-engineering matrix and scaffold based on newly devised multilayering and mixing electrospinning techniques. Biomaterials 2005;26:37-46.

37. Veis A, Anesey J, Cohen J. The long range reorganization of gelatin to the collagen structure. Archives of Biochemistry and Biophysics 1961;94:20-31.

38. Hulmes DJS, Miller A. Quasi-hexagonal molecular packing in collagen fibrils. Nature 1979;282:878-880.

39. Hulmes DJS, Holmes DF, Cummings C. Crystalline regions in collagen fibrils. Journal of Molecular Biology 1985;184:473-477.

40. Wess TJ, Hammersley AP, Wess L, Miller A. Molecular Packing of type I Collagen in Tendon. Journal of Molecular Biology 1998;275:255-267.

41. Prockop DJ, Fertala A. The Collagen Fibril: The Almost Crystalline Structure. Journal of Structural Biology 1998;122:111-118.

42. Gross J, Highberger JH, Schmitt FO. Collagen structures considered as states of aggregation of a kinetic unit. The tropocollagen particle. Proceedings of the National Academy of Sciences 1954;40:679-688.

43. Kadler KE, Holmes DF, Trotter JA, Chapman JA. Collagen fibril formation. Biochemical Journal 1996;316:1-11.

44. Chapman JA, Tzaphlidou M, Meek KM, Kadler KE. The collagen fibril--A model system for studying the staining and fixation of a protein. Electron Microscopy Reviews 1990;3:143-182.

45. Birk DE, Fitch JM, Babiarz JP, Doane KJ, Linsenmayer TF. Collagen fibrillogenesis *in vitro*: interaction of types I and V collagen regulates fibril diameter. Journal of Cell Science 1990;95:649-657.

46. Danielsen CC. Thermal stability of reconstituted collagen fibrils. Shrinkage characteristics upon *in vitro* maturation. Mechanics of Ageing and Development 1981;15:269-278.

47. Mentink CJAL, Hendriks M, Levels AAG, Wolffenbuttel BHR. Glucose-mediated cross-linking of collagen in rat tendon and skin. Clinica Chimica Acta 2002;321:69-76.

48. Hormann H, Schlebusch H. Reversible and irreversible denaturation of collagen fibers. Biochemistry 1971;10:932-937.

49. Kopp J, Bonnet M, Renou JP. Effect of collagen crosslinking on collagen-water interactions (a DSC investigation). Matrix (Stuttgart, Germany) 1989;9:443-450.

50. Bigi A, Panzavolta S, Rubini K. Relationship between triple-helix content and mechanical properties of gelatin films. Biomaterials 2004;25:5675-5680.

51. Tsereteli GI, Smirnova OI. Calometric study of the melting of gelatin gels. Polymer Science USSR 1991;33:2112-2118.

52. Zhang Z, Li G, Shi B. Physicochemical properties of collagen, gelatin, and collagen hydrolysate derived from bovine limed split wastes. Journal of the Society of Leather Technologists and Chemists 2006;90:23-28.

53. Raghunath M, Bruckner P, Steinmann B. Delayed Triple Helix Formation of Mutant Collagen from Patient with Osteogenesis Imperfecta. Journal of Molecular Biology 1994;236:940-949.

54. Zeugolis DI, Paul RG, Attenburrow G. Factors influencing the properties of reconstituted collagen fibres prior to self assembly: animal species and collagen extraction method. Journal of Biomedical Materials Research Part A In Press.

55. Cavallaro JF, Kemp PD, Kraus KH. Collagen Fabrics as Biomaterials. Biotechnology and Bioengineering 1994;43:781-791.

56. Wang M-C, Pins GD, Silver FH. Collagen fibres with improved strength for the repair of soft tissue injuries. Biomaterials 1994;15:507-512.

57. Huang L, Nagapudi K, Apkarian RP, Chaikof EL. Engineered collagen-PEO nanofibers and fabrics. Journal of Biomaterials Science Polymer Edition 2001;12:979-993.

58. Barnes CP, Pemble CW, Brand DD, Simpson DG, Bowlin GL. Cross-linking electrospun type II collagen tissue engineering scaffolds with carbodiimide in ethanol. Tissue Engineering 2007;13:1593-1605.

59. Highberger JH, Gross J, Schmitt FO. The interaction of mucoprotein with soluble collagen; An electron microscope study. Proceedings of the National Academy of Sciences 1951;37:286-291.

60. Gross J, Highberger JH, Schmitt FO. Extraction of collagen from connective tissue by neutral salt solutions. Proceedings of the National Academy of Sciences 1955;41:1-7.

61. Comper WD, Veis A. The mechanism of nucleation for *in vitro* collagen fibril formation. Biopolymers 1977;16:2113-2131.

62. Williams BR, Gelman RA, Poppke DC, Piez KA. Collagen fibril formation. Optimal in vitro conditions and preliminary kinetic results. Journal of Biological Chemistry 1978;253:6578-6585.

63. Holmes DF, Capaldi MJ, Chapman JA. Reconstitution of collagen fibrils in vitro; the assembly process depends on the initiating procedure. International Journal of Biological Macromolecules 1986;8:161-166.

64. Bear RS. The structure of collagen fibrils. Advanced Protein Research 1952;7:69-160.

65. Brodsky Doyle B, Hukins DWL, Hulmes DJS, Miller A, White S, Woodhead Galloway J. Low angle X-ray diffraction studies on stained rat tail tendons. Biochimica et Biophysica Acta (BBA) - Protein Structure 1978;535:25-32.

66. Hulmes DJS, Wess TJ, Prockop DJ, Fratzl P. Radial packing, order and disorder in collagen fibrils. Biophysical Journal 1995;68:1661-1670.

67. Campagnola PJ, Loew LM. Second-harmonic imaging microscopy for visualizing biomolecular arrays in cells, tissues and organisms. Nature Biotechnology 2003;21:1356-1360.

68. Williams RM, Zipfel WR, Webb WW. Interpreting Second-Harmonic Generation Images of Collagen I Fibrils. Biophysical Journal 2005;88:1377–1386.

69. Cox G, Kable E, Jones A, Fraser I, Manconi F, Gorrell MD. 3-Dimensional imaging of collagen using second harmonic generation. Journal of Structural Biology 2003;141:53-62.

70. Cox G, Xu P, Sheppard C, Ramshaw J. Characterization of the Second Harmonic Signal from Collagen. In: Periasamy A, So PT, editors. Multiphoton Microscopy in the Biomedical Sciences III: Proceedings of SPIE, 2003.

71. Stoller P, Reiser KM, Celliers PM, Rubenchik AM. Polarization-Modulated Second Harmonic Generation in Collagen. Biophysical Journal 2002;82:3330-3342.

72. Theodossiou TA, Thrasivoulou C, Ekwobi C, Becker DL. Second Harmonic Generation Confocal Microscopy of Collagen Type I from Rat Tendon Cryosections. Biophysical Journal 2006;91:4665–4677.

73. Kim B-M, Eichler J, Reiser KM, Rubenchik AM, Da Silva LB. Collagen structure and nonlinear susceptibility: Effects of heat, glycation, and enzymatic cleavage on second harmonic signal intensity. Lasers in Surgery and Medicine 2000;27:329-335.

74. Usha R, Ramasami T. The effects of urea and n-propanol on collagen denaturation: using DSC, circular dicroism and viscosity. Thermochimica Acta 2004;409:201-206.

75. Chu FH, Lukton A. Collagenase Induced Changes in the Circular Dichroism Spectrum of Collagen. Biopolymers 1974;13:1427-1434.

76. Brodsky-Doyle B, Leonard KR, Reid KBM. Circular-Dichroism and Electron-Microscopy Studies of Human Subcomponent C1q before and after Limited Proteolysis by Pepsin. Biochemical Journal 1976;159:279-286.

77. Jenness DD, Sprecher C, Johnson JWC. Circular Dichroism of Collagen, Gelatin, and Poly(proline) II in the Vacuum Ultraviolet. Biopolymers 1976;15:513-521.

78. Bruckner P, Prockop DJ. Proteolytic enzymes as probes for the triple-helical conformation of procollagen. Analytical Biochemistry 1981;110:360-368.

8. Figure legends

Figure 1. SEM micrographs of the produced scaffolds. A, D and G: self-assembled fibres derived from in-house, Koken and Symatese collagen respectively. B, E and H: electro-spun nano-fibres derived from in-house, Koken and Symatese collagen respectively dissolved in HFP. C: extruded in-house collagen derived micro-fibre; insert: native rat-tail tendon fibre. F: electro-spun nano-fibres derived from Koken collagen dissolved in TFE. I and L: electro-spun nano-fibres derived from Symatese collagen-mPCL and Sigma gelatin B-mPCL dissolved in HFP. J and K: electro-spun nano-fibres derived from Sigma gelatin B and mPCL respectively dissolved in HFP.

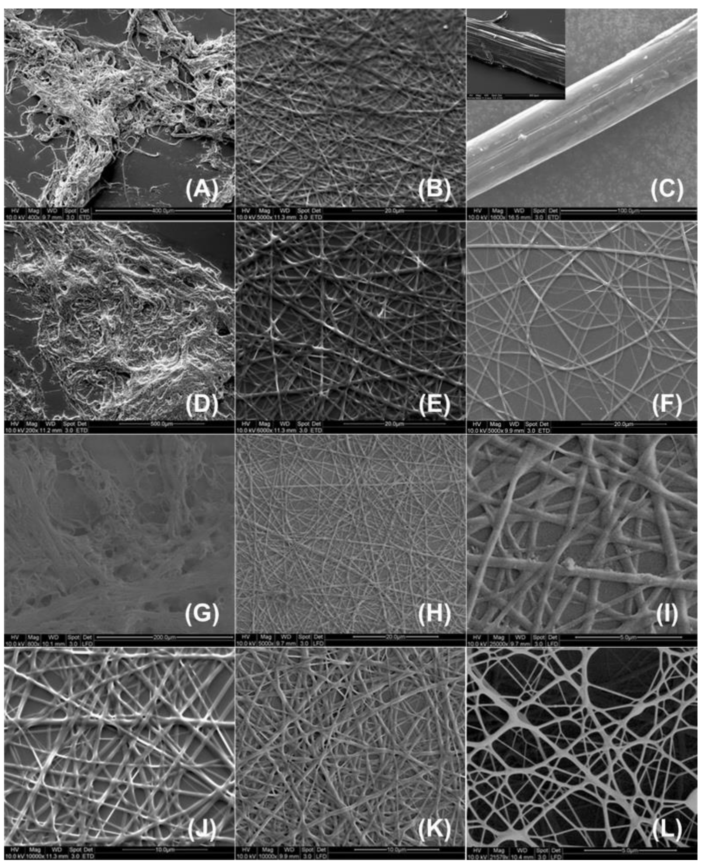

Figure 2. TEM micrographs of: A and E; B and F; C and G: self-assembled fibres derived from in-house, Koken and Symatese collagen respectively; I and M; J and N; K and O: self-assembled fibres derived from HFP-recovered in-house, Koken and Symatese collagen respectively; Q and U; R and V; S and W: electro-spun nano-fibres originated from in-house, Koken and Symatese collagen respectively dissolved in HFP; D and H: extruded in-house collagen derived micro-fibres; L and P: native rat-tail tendon; T and X: electro-spun nano-fibres originated from Koken collagen dissolved in TFE. The quarter-stagger arrangement of collagen was apparent for self-assembled, extruded and native rat tail tendon fibres, inconsistent for the HFP-recovered self-assembled fibres and not-existent for the electro-spun nano-fibres, independent of the solvent.

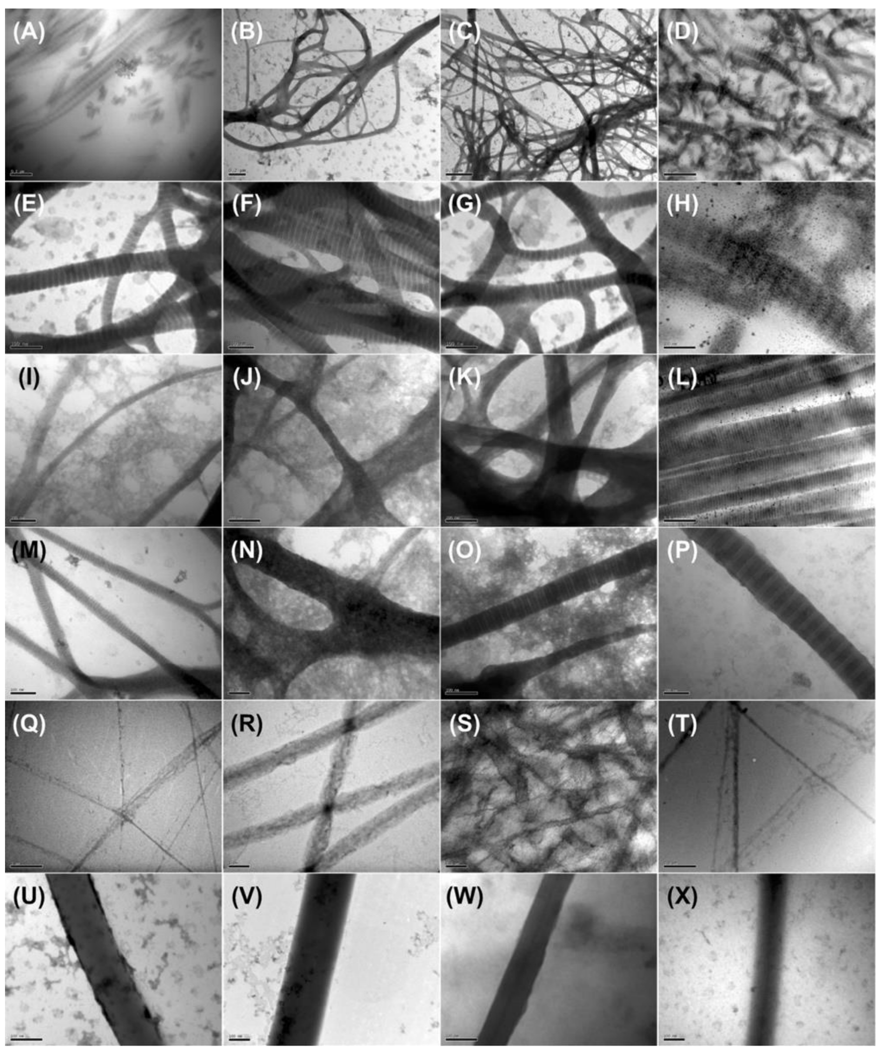

Figure 3. Bright-field and corresponding second harmonic generation images for: (a & e) human normal skin; (b & f) rat tail tendon; (c & g) in-house freeze-dried collagen; (d & h) extruded in-house collagen micro-fibres; (i & m) in-house HFP-recovered freeze-dried collagen; (j & n) electro-spun nano-fibres derived from Koken collagen using HFP; (k & o) electro-spun nano-fibres derived from Koken collagen using TFE; and (l & p) electro-spun nano-fibres derived from blend of Symatese collagen and mPCL using HFP. Electro-spun nano-fibres failed to exhibit SHG signals, in contrast to any other collagenous structure.

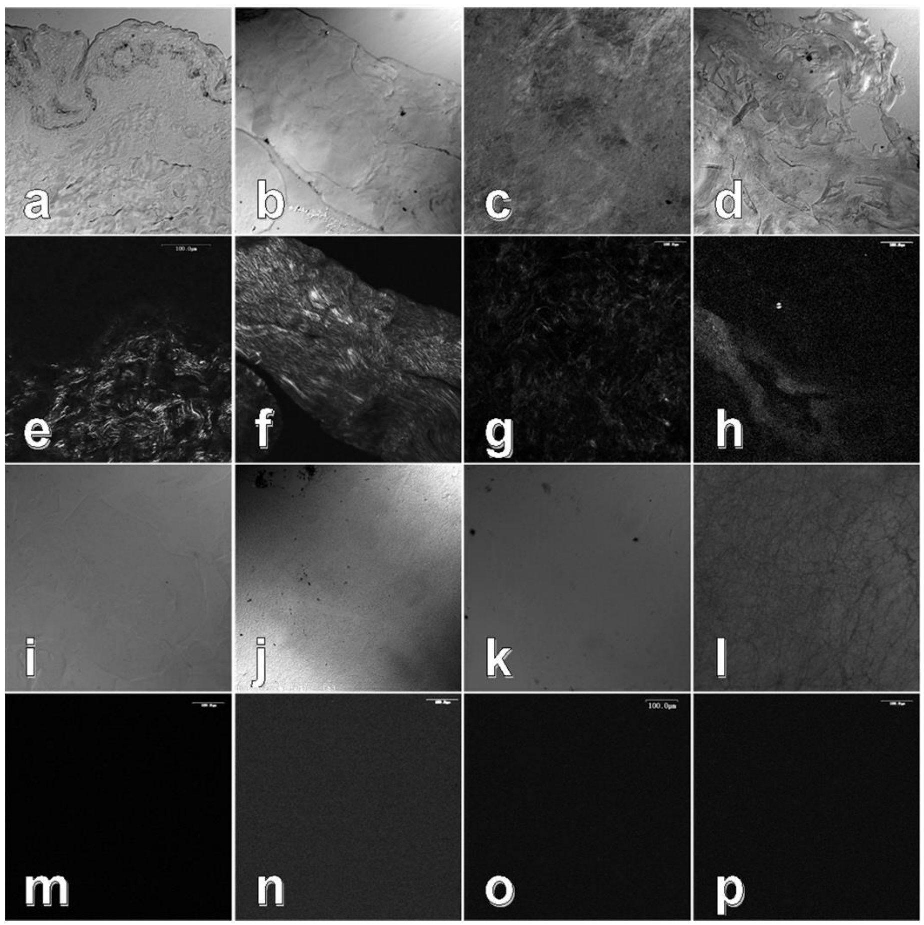

Figure 4. CD spectra of the acid-solubilised (left column) and the pepsin-digested (right column) materials plotted as mean residue ellipticity [10^{-4} x (deg x cm^2 x $dmol^{-1}$)] Vs wavelength (nm). Typical spectra were obtained from the freeze-dried collagens and gelatin, indicating the presence and the lack of triple-helical structure respectively. The electro-spun collagen derived nano-fibres and the HFP-recovered collagen exhibited random-coil transitions similar to those obtained from the gelatin preparations or charged polypeptides.

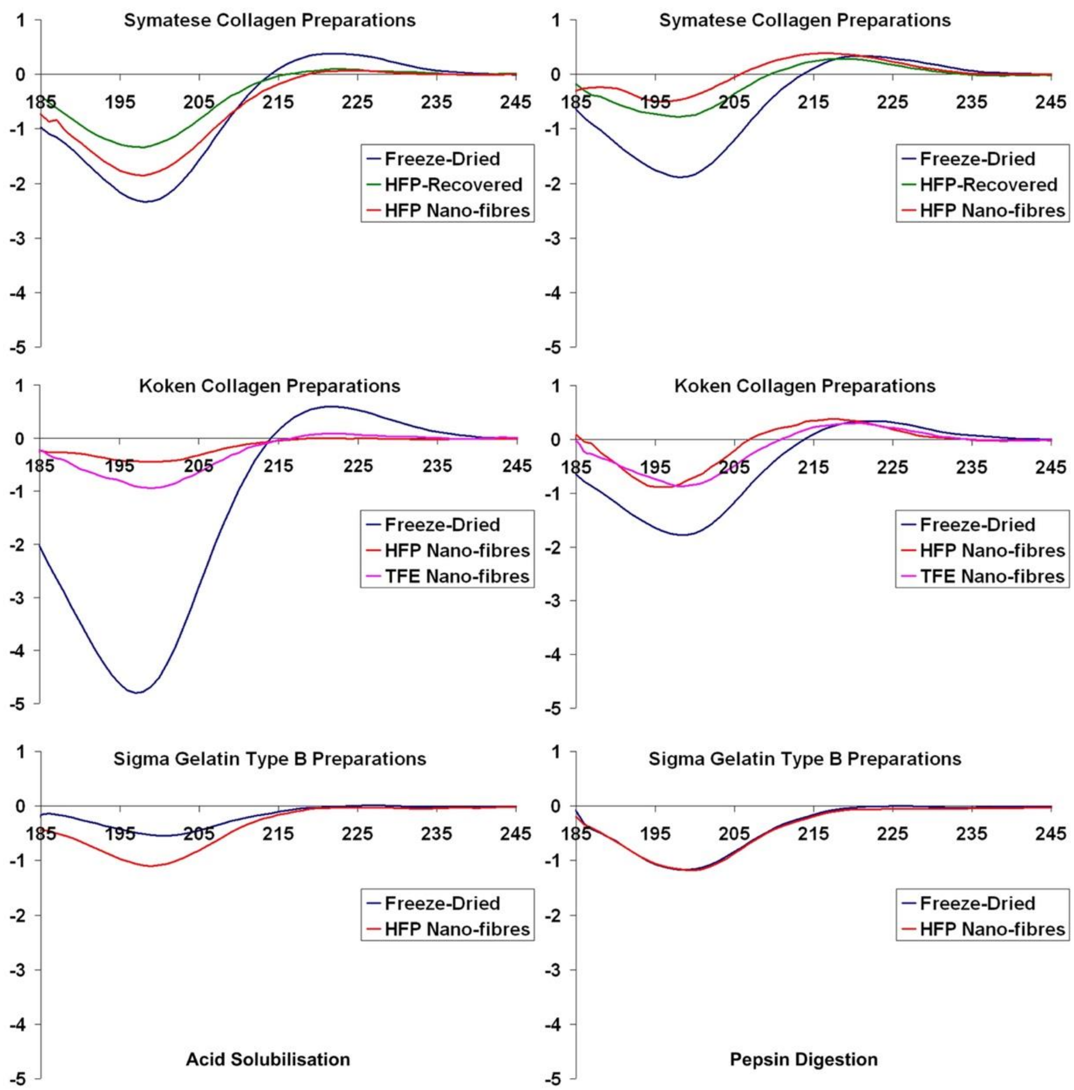

Figure 5. SDS-PAGE analysis of acid-solubilised and corresponding pepsin-digested materials: (a & c) freeze-dried Sigma gelatin type B; (b & d) Sigma gelatin type B electro-spun nano-fibres; (e & h) freeze-dried Symatese collagen; (f & i) HFP-recovered Symatese collagen; (g & j) Symatese collagen electro-spun nano-fibres. The results demonstrate reduction in collagen content after disassociation in HFP and even greater losses after electro-spinning.

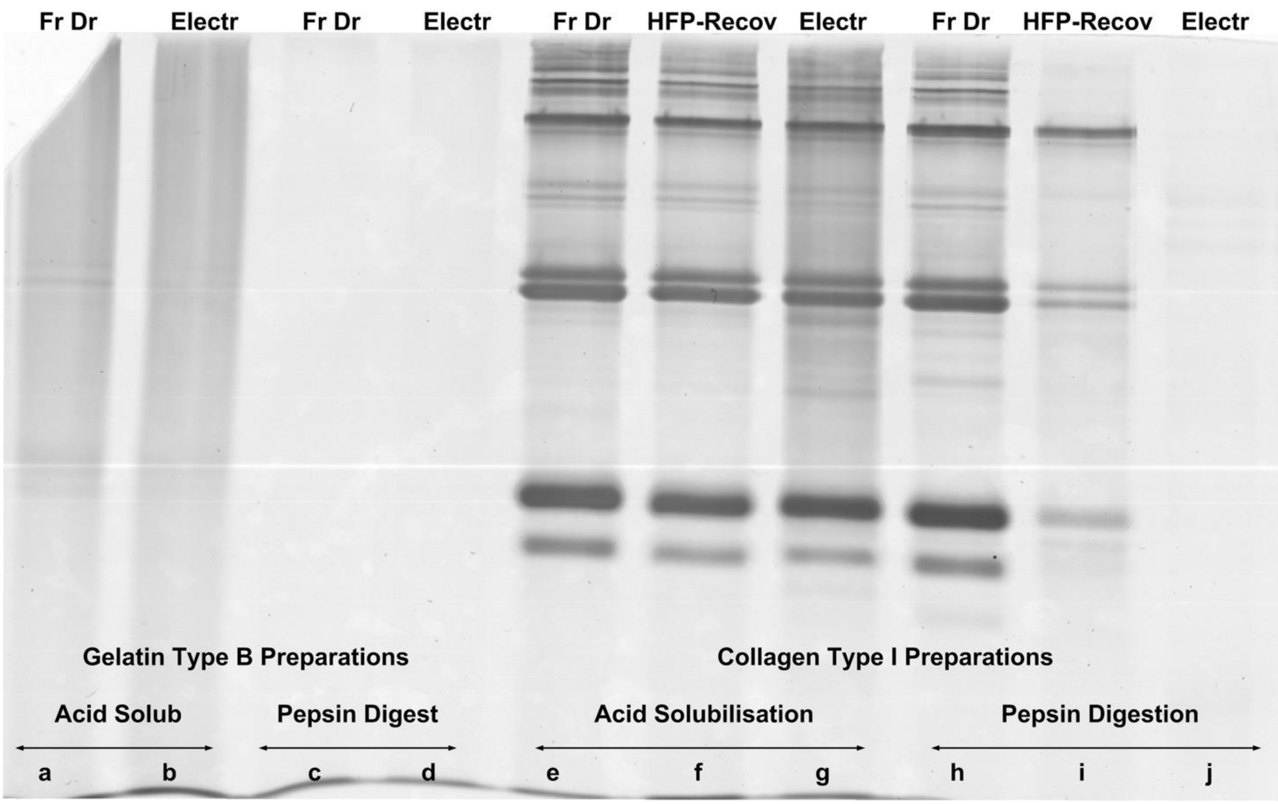

Figure 6. SDS-PAGE analysis of acid-solubilised and complementary pepsin-digested in-house collagen preparations: freeze-dried collagen (a & e); HFP-recovered collagen (b & f); extruded collagen fibres (c & g); electro-spun collagen-originated nano-fibres (d & h).

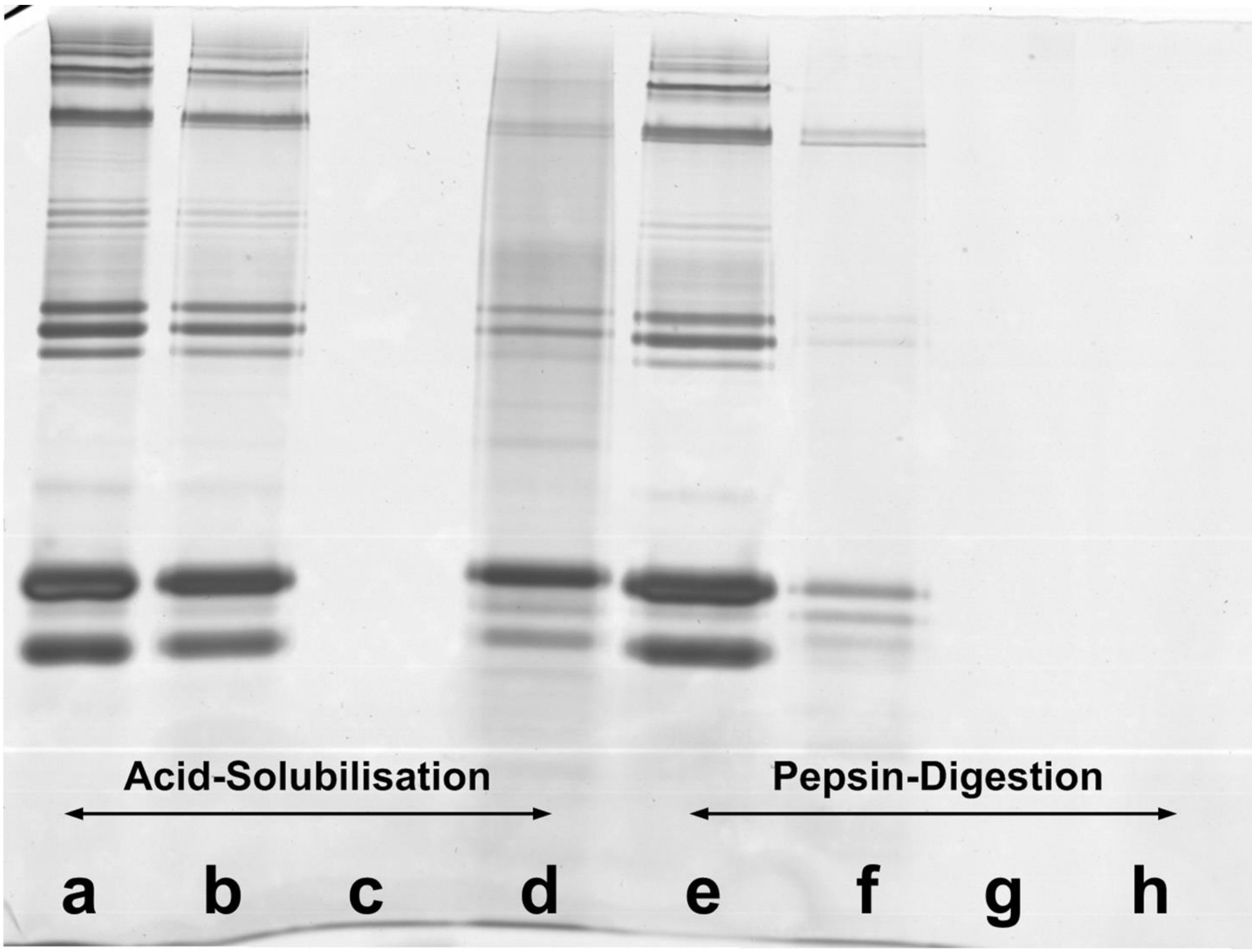

Figure 7. SDS-PAGE analysis of acid-solubilised and analogous pepsin-digested Koken collagen preparations: freeze-dried collagen (a & d); HFP-derived electro-spun nano-fibres (b & e); TFE-derived electro-spun nano-fibres (c & f).

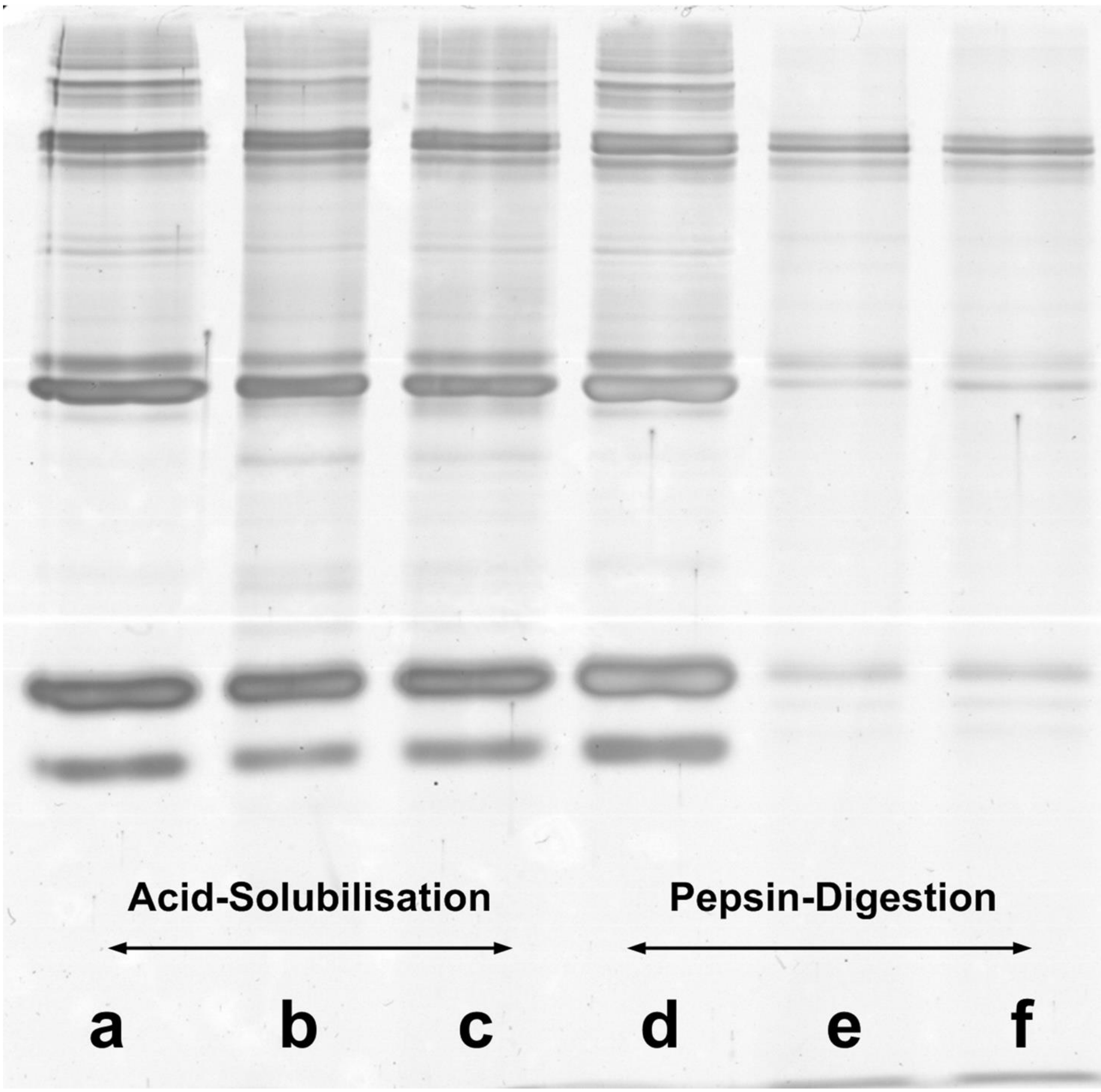

Figure 8. SDS-PAGE analysis of acid-solubilised and pepsin-digested: freeze-dried Symatese collagen preparation (a & h); freeze-dried Sigma gelatin type A (b & i and e & l); electro-spun nano-fibres of mPCL-Gelatin type A (c & j and f & m); electro-spun nano-fibres of mPCL-Symatese collagen (d & k and g & n). 0.5μg/well of protein were loaded for the a to d and h to k samples, whilst 1.0μg/well of protein were loaded for the e to g and l to n samples.

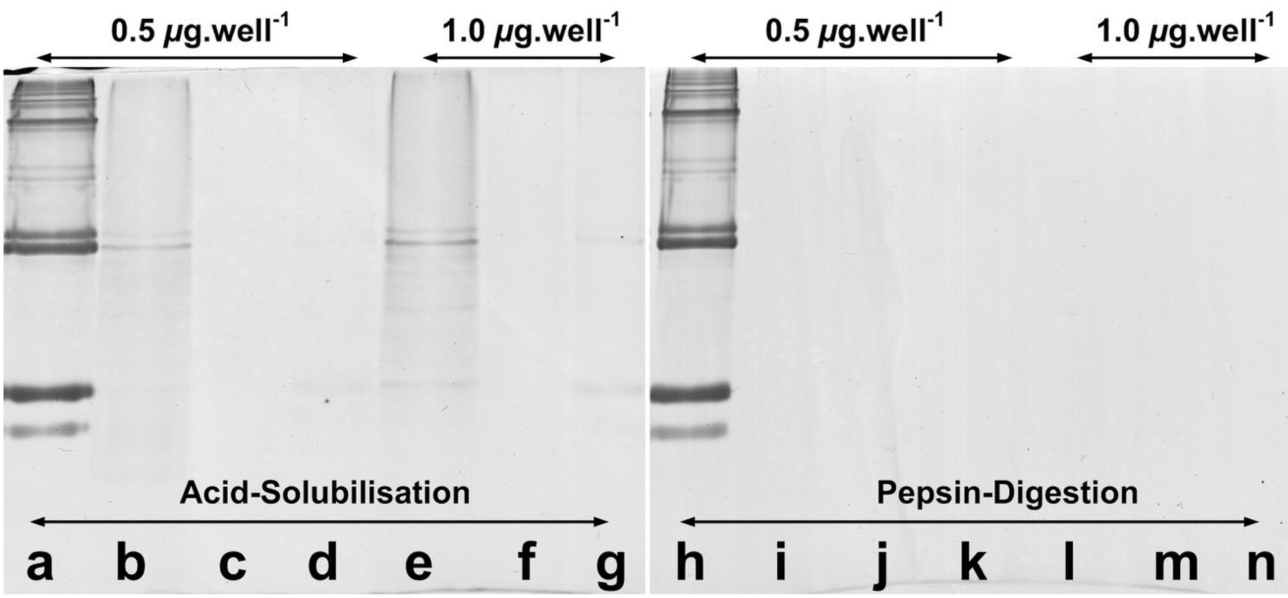

9. Table legends

Table 1. DSC results of wet tested materials. Three replicates were carried out for every sample, but the native rat tail tendon for which four replicates were carried out. ±: indicates standard deviation.

Sample Description		ΔH_D (J/g)	Onset (^{0}C)	Peak (^{0}C)
	Freeze-Dried	-4.96±0.52	47.21±0.73	53.19±0.17
	HFP-Recovered	-1.63±0.13	37.07±0.91	40.36±0.16
In-House Collagen	Electro-spun Fibres	-1.64±0.38	29.35±2.50	37.39±0.20
	Extruded Fibres	-14.24±1.74	50.50±0.69	55.52±0.47
	Freeze-Dried	-3.15±0.86	47.61±1.75	52.04±0.53
Symatese Collagen	HFP-Recovered	-0.98±0.22	34.22±2.02	38.35±1.08
	Electro-spun Fibres	-1.41±0.45	31.94±3.29	36.61±1.03
	Freeze-Dried	-3.81±0.40	43.59±0.44	49.85±0.48
Koken Collagen	Electro-spun Fibres HFP	-1.33±0.32	35.82±0.97	40.05±1.04
	Electro-spun Fibres TFE	-2.11±0.82	34.74±1.28	39.71±1.44
Sigma Gelatin B	Freeze-Dried	-2.29±0.07	27.24±4.24	33.33±0.57
	Electro-spun Fibres	-0.73±0.19	29.73±1.55	34.15±0.83
PCL	Raw material	-73.65±2.12	53.02±0.65	64.33±1.43
	Electro-spun Fibres	-23.21±5.84	51.76±0.15	54.14±0.21
Electro-spun fibrous Blends	PCL-Symatese Collagen	-11.24±0.77	51.72±0.53	53.97±0.11
	PCL-Sigma Gelatin B	-6.51±0.49	52.45±0.50	54.99±0.45
Native rat tail tendon Fibres		-14.06±1.00	58.28±1.07	63.16±1.44

Table 2. Quantitative evaluation of the SDS-PAGE (Figure 5) of Symatese collagen structures after exposure to HFP and after electro-spinning.

Symatese collagen	Freeze-Dried Adj. Vol. (OD*mm^2)	HFP-Recovered Adj. Vol. (OD*mm^2)	Electro-spun Fibres Adj. Vol. (OD*mm^2)
Acid-Solubilisation α1(I)	5.457	4.451	4.734
Acid-Solubilisation α2(I)	1.569	0.944	0.770
Pepsin-Digestion α1(I)	5.640	0.593	0.036
Pepsin-Digestion α2(I)	1.661	0.058	0.006